http://dx.doi.org/10.5012/bkcs.2013.34.7.2111

Substituent Effects on Conformational Changes in (+)-CSA Doped Polyaniline Derivatives

Eung Lee and Eunok Kim*

*Department of Chemistry, The University of Suwon, Hwaseong-si, Gyeonggi-do 445-743, Korea. *E-mail: eokim@suwon.ac.kr*
Received March 21, 2013, Accepted April 22, 2013

This paper reports substituent effects on the conformational changes in polyaniline (PAni) derivatives. PAni, poly-*o*-toluidine (POT), and poly-*o*-anisidine (POA) were formed by potentiodynamic electropolymerization in aqueous solution containing (+)-camphorsulfonic acid (CSA) as a dopant. UV-Vis spectroscopy and cyclic voltammetry measurements revealed that the methyl group showed a greater steric hindrance than the methoxy group. Further, the doping level decreased with increasing steric hindrance. The sign pattern of the circular dichroism (CD) bands for POA was opposite to that for PAni. However, no CD bands were observed in POT. The steric hindrance caused helical inversion, but at a high level of steric hindrance, the helical conformation could not be adopted, because of the reduced doping level. The reduced crystallinity was greatly affected by the decreased doping level. The steric effect influenced the polymer conformation and the doping level, thus determining the optical activity, morphology, and crystallinity of the PAni derivatives.

Key Words : Conducting polymers, Polyaniline derivatives, Chirality, Steric effect, Electropolymerization

Introduction

Chiral conducting polymers have attracted much attention because of their potential applications as chiral catalysts for asymmetric hydrogenation,[1] chiral electrodes for electrochemical asymmetric synthesis,[2] chiral sensors for the selective detection of chiral molecules,[3,4] and chiral stationary phases for the separation of enantiomers.[5,6] Majidi *et al.*[7] and Havinga *et al.*[8] were the first to synthesize optically active polyaniline (PAni) by the electrochemical polymerization of aniline in the presence of (+)- or (−)-camphorsulfonic acid (CSA) as a chiral dopant. Ashraf *et al.* proposed that chiral induction results from electrostatic interactions between the sulfonate anion in CSA and the radical cation NH^{+} in aniline, and hydrogen bonding between the carbonyl group in CSA and the NH sites on the PAni chains.[9]

Optically active PAni derivatives have been synthesized by the introduction of a substituent (*e.g.*, methyl, methoxy) into the phenyl ring,[10,11] covalent attachment of a substituent to the N centers,[12] or copolymerization of aniline with its derivatives.[13-15] Change in the optical activity of PAni derivatives is one of the important challenges in academics and potential applications. Poly-*o*-toluidine (POT) doped with (+)-CSA (POT/(+)-CSA) does not adopt a helical conformation with a predominantly one-handed screw sense, because attachment of the chiral CSA^{-} ions to the $NH^{\bullet+}$ and NH centers is sterically blocked by the methyl groups.[16] On the other hand, the helicity of the poly(aniline-*co*-*m*-toluidine)/(+)-CSA copolymer is inverted with respect to that of PAni because of the handedness inversion of the N-H terminus.[13] According to Su *et al.*, the alkyl or alkoxy group in chiral PAni derivatives may inhibit electrostatic interactions and hydrogen bonding between the derivative backbone and the chiral dopant. Further, solvent-induced changes in the degree of electrostatic interaction can affect the helical conformation.[11] Substituent-induced conformational changes can also affect the crystallinity of PAni. The arrangement of polymer chains would vary depending on the presence of the substituent in the phenyl ring of PAni. When bulky substituents are introduced in PAni, the arrangement of polymer chains becomes irregular, which then decreases the crystallinity.[17] Therefore, the order of crystallinity increases with the regularity in the arrangement and ordering of the polymer chains.[18]

In this study, PAni, POT, and poly-*o*-anisidine (POA) films were formed by potentiodynamic electro-polymerization in aqueous solution containing (+)-CSA as a dopant. We have investigated that the steric effect of a substituent affects the conformation of the polymeric backbone and the doping level. Eventually, these conformation and doping level greatly influenced the optical activity, morphology and crystallinity of PAni derivatives.

Experimental

(+)- and (−)-CSA, *o*-anisidine, and *o*-toluidine (Aldrich chemicals) were used as supplied. Aniline (Duksan Chemicals) was purified by distillation before use. All aqueous solutions were prepared using deionized water (> 18.2 MΩ). Aqueous solutions of the desired monomer (0.1 M) and (+)-CSA (0.5 M) were used as the supporting electrolyte. Prior to the experiment, nitrogen gas was flushed through the electrochemical cell and polymerization solution to remove any dissolved oxygen from the electrolyte. Deposition and electrochemical measurements were performed using a WBCS3000 battery cycler system (WonATech, Korea). A three-electrode system comprising an indium tin oxide (ITO) working electrode, a Ag/AgCl (3 M NaCl) reference elec-

trode, and a platinum plate counter electrode was used. To obtain the desired amount of data, electrodeposition was carried out under potentiodynamic conditions over the voltage range 0.0-1.1 V, at a scan rate of 10 mV/s for 20 or 40 cycles. UV-Vis spectra of the polymers in dimethyl sulfoxide (DMSO) solution were recorded using an S-3100 spectrophotometer (Scinco) over the wavelength range 300-1100 nm, in order to determine the conformational changes in the polymer chains. Then, the dopants were removed by treatment with 0.1 M NH_4OH to form de-doped polymer films. Changes in the chemical structure of the polymers were determined on the basis of Fourier transform infrared (FT-IR) spectra recorded using an FT-IR 4100 spectrometer (Jasco) with an PRO 470-H attenuated total reflection (ATR) single-reflection accessory. To elucidate the polymer conformation, circular dichroism (CD) spectra were recorded in DMSO using a J-815 spectropolarimeter (Jasco) in DMSO, over the range 300-800 nm at a scan rate of 200 nm/min. The morphology of the films was studied by scanning electron microscopy (SEM; VEGA 3 LMU, Tescan; acceleration voltage: 20 kV) after coating the surfaces with Pt. The structural properties were examined by X-ray diffraction (XRD; DMAX-2200, Rigaku) using Cu Kα radiation, at 40 kV and 40 mA. XRD data were recorded over the 2θ range 15°-30°.

Result and Discussion

Cyclic Voltammetry. While both potentiostatic and potentiodynamic methods have been widely used for the electropolymerization of chiral PAni, the latter is more advantageous for the preparation of PAni films. Potentiostatically prepared films tend to exhibit a relatively rough surface and low density because of the hindered diffusion along the interface. However, the films prepared by the potentiodynamic method are uniformly dense and smooth and are well adherent to the ITO electrode.

Figures 1(a), (b), and (c) show the cyclic voltammograms recorded during potentiodynamic growth of PAni, POA, and POT on ITO. The oxidation peaks observed in the first cycle corresponded to the oxidation of monomers, which produce radical cations. Three clear oxidation peaks, which could be assigned to the electrochemical oxidation of the deposited polymer and any intermediate species, appeared after the fifth cycle. The current corresponding to the redox peaks gradually increased with the number of cycles, indicating the growth of polymer films in each cycle[19]; the current decreased in the order PAni > POA > POT, because polymerization was inhibited by the steric hindrance from the bulky substituent in the PAni derivatives. Thus, the thicknesses of these polymer films followed the order: PAni > POA > POT. Figure 1(d) shows the cyclic voltammograms in the fifth cycle for PAni, POA, and POT.

The first (180 mV) and last (770 mV) oxidation peaks for PAni were due to the successive oxidation of leucoemeraldine to emeraldine and emeraldine to pernigraniline, respectively. The middle oxidation peak at 460 mV was most probably due to quinone intermediates or the formation of

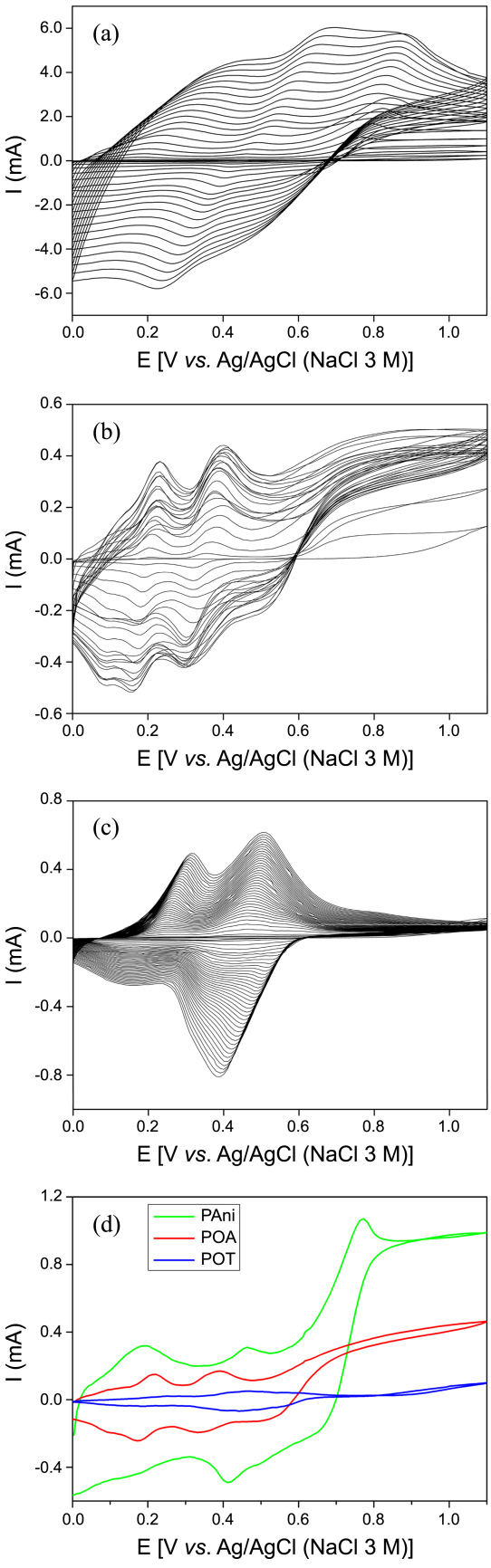

Figure 1. Cyclic voltammograms recorded during film growth: (a) PAni (20 cycles), (b) POA (20 cycles), (c) POT (40 cycles), and (d) PAni, POA, and POT in the 5th cycle.

cross-linked PAni chains.[20] Electron-donating substituents such as methyl or methoxy at the *ortho* position of the phenyl ring may facilitate easy oxidation of the polymer, and hence, the oxidation peaks would shift in the negative direction (electronic effect). However, the bulky substituents could increase the torsion angle between adjacent rings to relieve steric strain and result in a nonplanar conformation, thus decreasing the conjugation length along the polymer backbone (steric effect).[21] The first oxidation peak (220 mV) of POA shifted toward a positive potential as compared to that of PAni, indicating that the steric effect plays a more dominant role than the electronic effect. The first oxidation peak of POT shifted to a more positive potential (250 mV) as compared to that of POA because of the large steric hindrance and weak electron-donating effect of the methyl group.

The last oxidation peaks of the methyl- or methoxy-substituted PAni shifted toward a negative potential as compared to that of PAni, probably because of the prominent electronic effect of the substituent. Oxidation of the radical cation formed on the polymer backbone to the imide form must be facilitated by the presence of the sp^2 hybridized nitrogen; this would diminish the steric strain due to the wide dihedral angle, while maintaining the electronic effect of the substituent. Therefore, the oxidation potential of the emeraldine to pernigraniline transition decreased in POA and POT films.[22]

FT-IR Spectra. Figure 2 shows the FT-IR/ATR spectra of the (+)-CSA-doped PAni, POA, and POT films. The structures of POA and POT were confirmed form the characteristic FT-IR peaks of PAni and CSA. PAni showed absorption peaks at around 1600, 1500, 1120, 1100, and 790 cm^{-1}. The peak at 1600 cm^{-1}, assigned to C-C stretching and C=N stretching vibrations of the quinoid ring, and that at 1500 cm^{-1}, attributed to C-C stretching in the benzenoid ring, confirmed the presence of amine and imine units.[23] The peaks at 1120, 1100, and 790 cm^{-1} were due to in-plane C-H bending vibrations, aromatic C-H vibrations, and out-of-plane

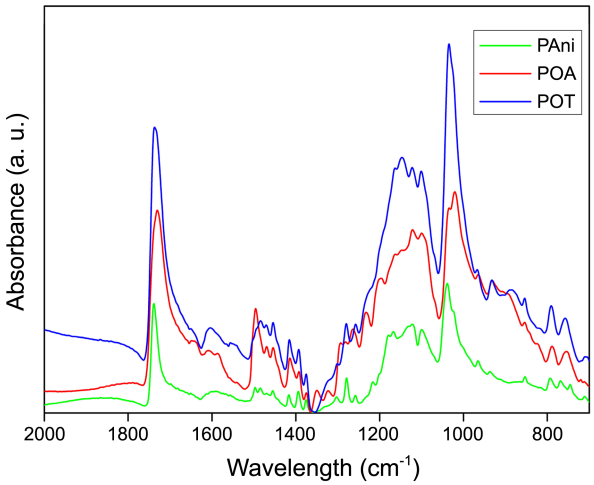

Figure 2. FT-IR/ATR spectra of PAni, POA, and POT doped with (+)-CSA.

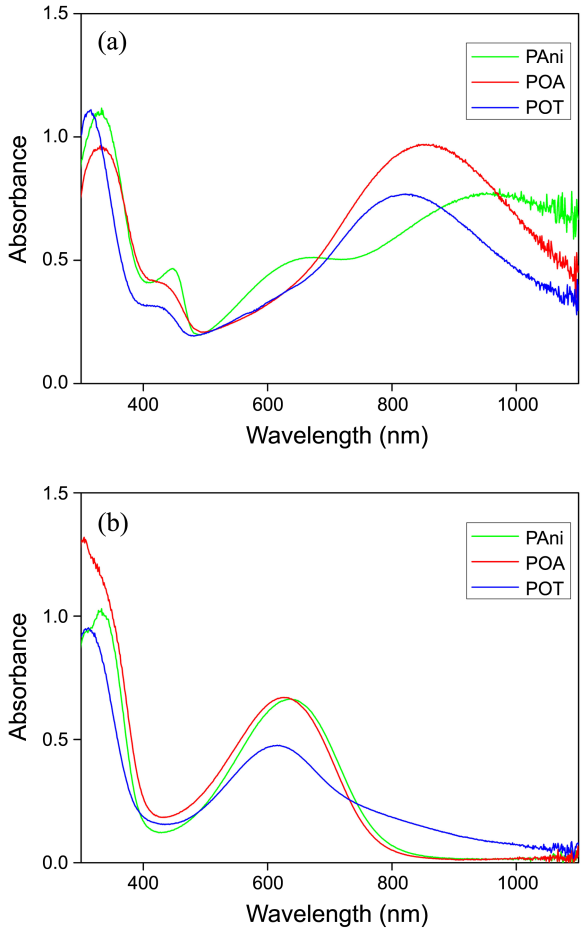

Figure 3. UV-Vis spectra of PAni, POA, and POT in the doped (a) and de-doped (b) states.

C-H bending vibrations, respectively. The peaks at 1740 and 1040 cm^{-1} indicated the presence of CSA. The peaks at 1740 and 1035 cm^{-1} were assigned to C=O stretching[24] and the $-SO_3$ group, respectively.[15] The main differences between the spectra of PAni and its derivatives were as follows. POT showed a peak at 880 cm^{-1}, which could be assigned to the methyl group attached to the phenyl ring,[25] while POA showed peaks at 1264 and 1021 cm^{-1}, which corresponded to C-O-C stretching of the alkyl-aryl ether linkage resulting from the presence of *o*-methoxy groups.[26]

UV-Vis Spectra. The UV-Vis spectra of PAni, POA, and POT in the doped and de-doped states are shown in Figure 3. Doped PAni showed three characteristic bands: 335 nm, due to $\pi \rightarrow \pi^*$ transition in the benzenoid rings; 450 nm, due to polaron $\rightarrow \pi^*$ transition; and 960 nm, due to $\pi \rightarrow$ polaron transition in the emeraldine salt form of doped PAni.

The de-doped PAni showed an absorption band attributable to $\pi \rightarrow \pi^*$ transition at 330 nm. Further, the excitonic transition at 630 nm was due to $n \rightarrow \pi^*$ transition from the non-bonding nitrogen lone pair to the conduction band. In the spectrum of doped POA, a band assigned to the $\pi \rightarrow \pi^*$ transition in the benzenoid rings appeared at 335 nm, as in the case of PAni. However, the polaron absorption bands blue-shifted to 430 and 850 nm as compared to those of PAni

(at 450 and 960 nm). An electron-donating substituent can make the electronic environment in the backbone different from that in the parent PAni, resulting in increased localized electron density. In addition, steric effects between the substituent and the hydrogen on the adjacent nitrogen atom can result in highly twisted polymer chains.[27]

As shown in Figure 3(a), the spectrum of doped POT was blue-shifted as compared to that of PAni, probably because of the dominance of the steric effect over the electronic effect. Further, the band gap of the derivatives increased because of the increased torsion angle between the C-N-C plane and the benzene ring plane.[15] In the case of the doped PAni derivatives, the intensity of the peaks at around 430 nm ($\pi \rightarrow \pi^*$ transition) decreased because of the change in the doping level and polaron formation.[28] The absorption spectra indicated that the electrostatic interactions between the polymer chains and the dopants are interrupted by the substituent, thus resulting in a decreased doping level. The conformational changes in POT were more extensive than those in doped POA, because POT showed a more blue-shifted spectrum and decreased doping level.

This result indicated that the steric hindrance caused by the methyl group is greater than that caused by the methoxy group. This behavior can be explained by the smaller van der Waals radius of the oxygen atom (1.40 Å) than that of the methyl group (2.00 Å). In POT, the substituent is linked to the phenyl ring by the carbon atom. However, in POA, the substituent is linked *via* the oxygen atom, which reduces the steric strain.[29] These results show that the conjugation length and doping level are directly related to the nature of the substituent atom linked to the phenyl ring in PAni.

Circular Dichroism Spectra. Mirror-image CD spectra were observed for PAni/(+)-CSA and PAni/(−)-CSA in the UV-Vis region (Figure 4), indicating enantioselective acid doping of PAni with the chiral CSA. The polymer chains would preferentially adopt a one-handed helical conformation depending on the hand of the CSA ion incorporated during polymerization.[30] The CD band due to the CSA^- ion (290 nm) and the bands attributed to the polymer backbone

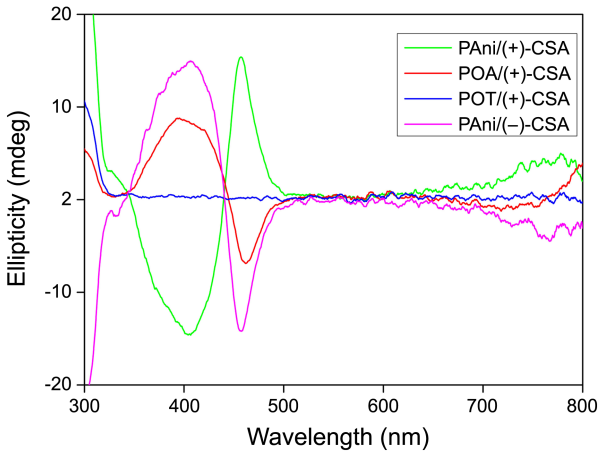

Figure 4. CD spectra of PAni, POA, and POT doped with (+) or (−)-CSA, in DMSO solution.

(330, 400, 460, and 780 nm) indicated the chiral structure of the polymer chains. The CD bands at 400 and 460 nm could be assigned as the bisignate exciton-coupled bands associated with the polaron $\rightarrow \pi^*$ transition observed at 450 nm.[10] The broad band centered at 780 nm was associated with the localized polaron absorption band. The sign pattern of the polaron absorption bands for POA/(+)-CSA was opposite to that for PAni/(+)-CSA.

There are some reports on the inversion of helical chirality by the substituent on the phenyl ring in PAni. According to Yan *et al.*, when a chiral (+)-CSA dopant is used, aniline reacts with the N-H terminus on the left-hand side all along the polymer chains, thus yielding a right-handed chiral helix for PAni/(+)-CSA during polymerization. However, the methyl group on the phenyl ring directly affects the approach direction of the monomers, thus inverting the chirality of the N atom near the reaction site in the poly(aniline-*co*-*m*-toluidine)/(+)-CSA copolymer.[13] Yuan *et al.* also showed that helical inversion originated from the dynamic switch between electrostatic interactions and hydrogen bonding. The main dynamic for helical induction is the electrostatic interaction between the NH^+ cation of PAni and the SO_3^{-2} ion of β-cyclodextrin sulfate (CDS). However, when the electrostatic interactions are interrupted by a methoxy substituent in the phenyl ring of PAni, hydrogen bonding between the NH hydrogen of POA and the SO_3^{-2} oxygen of CDS would be the main dynamic to helical induction in POA/CDS. Thus, the preferential interaction between the molecules changes gradually with the chemical environment.[10]

In POT/(+)-CSA, only the (+)-CSA absorption band at 290 nm was observed, and no bands for the polymer backbone could be seen, because of the decreased doping level The decreased doping level did not cause chiral induction into POT chains, indicating that the polymer probably were not arranged in one-handedness, because the strong steric hindrance of methyl group disturb the incorporation of CSA^- ion into a polymer.

Scanning Electron Microscopy. SEM images (Figure 5) revealed that the films were compact and uniformly deposited on the ITO electrode. The SEM image of PAni recorded after 20 cycles under 10 kx magnification (Figures 5(a)) revealed a rod-like morphology. Since CSA^- ion has surfactant-like properties, micelle formation can occur in aqueous solution because of the hydrophobicity of the monomers and the hydrophilicity of CSA (*e.g.*, $-SO_3^-$ group).[31] The micelles acted as soft templates during polymerization; hence, the polymer chains had well-ordered structures. In addition, at a high (+)-CSA/monomer molar ratio of 5:1, the excess (+)-CSA prevented the aggregation of PAni nuclei during polymerization, resulting in a well-ordered structure.[32]

The morphology of the PAni derivative may be strongly influenced by the substituent[19]; the well-ordered granular structure of POA could be attributed to the steric hindrance from the bulky methoxy groups. The SEM image of POT recorded after 20 cycles under 5 kx magnification is shown in Figure 5(c). The methyl group restricted the polymer

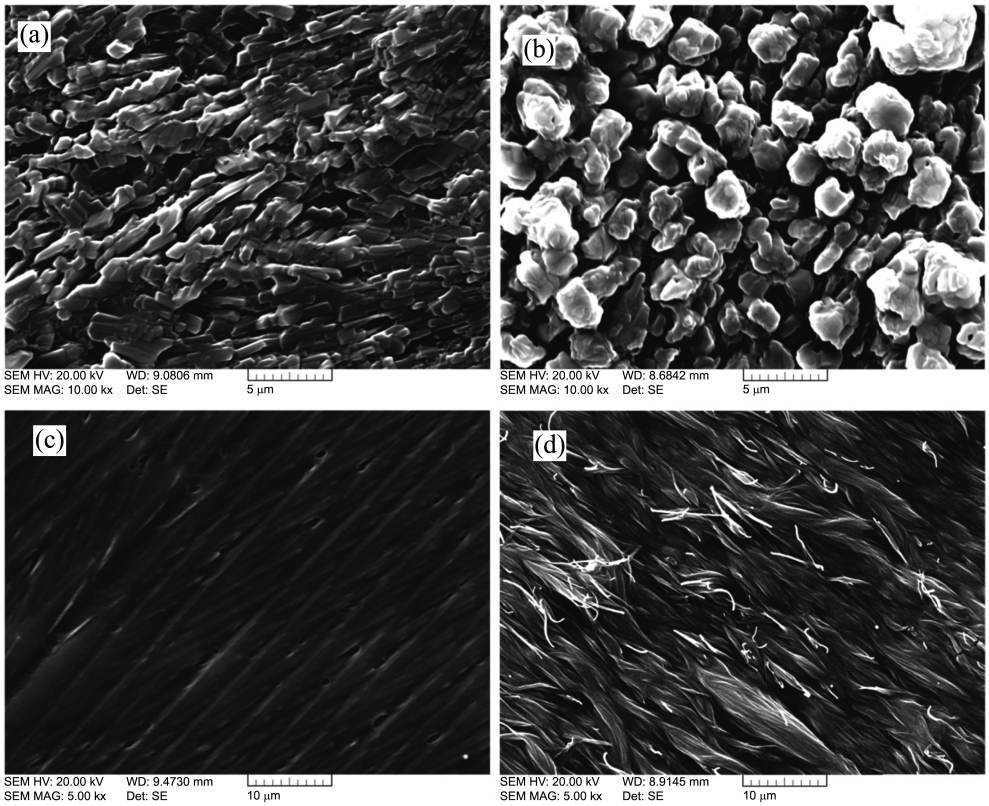

Figure 5. SEM images of (a) PAni (20 cycles; 10 kx), (b) POA (20 cycles; 10 kx), (c) POT (20 cycles; 5 kx), and (d) POT (40 cycles; 5 kx).

growth, resulting in a thin POT film. The obvious difference between the SEM images of POA and POT was due to the increased steric hindrance by the methyl group as compared to that by the methoxy group (Figures 5(b) and (c)). To obtain the desired amount of the data for the steric hindrance-induced morphological changes in POT, the number of electropolymerization cycles was increased from 20 to 40. The SEM images recorded after 40 cycles under 5 kx magnification revealed the fibrous structure of POT (Figure 5(d)). Thus, SEM analysis showed a morphological change from the rod-like PAni to the granular POA and fibrous POT.

X-ray Diffraction. Figure 6 shows the XRD patterns of the (+)-CSA-doped PAni, POA, and POT deposited on the ITO electrode. The peaks at 2θ = 18.66 and 19.44° could be attributed to CSA in the PAni derivative samples.[33] The sharp peaks for the polymer chains of PAni were observed at 2θ = 15.22 (intra-chain ordering within the PAni molecules), 21.18 (inter-chain stacking distance between phenyl rings) and 27.4°.[33-35] Based on this, it seems that the chiral CSA highly influenced the increase in crystallinity. The sharp diffraction peaks of PAni and POA indicated that the majority of the polymer chains were ordered in the crystal planes. It seems that the increased crystallinity is due to the ordered helical structure in the polymer backbone. However, there was no clear indication for the existence of crystalline phases in POT. Since the strong steric hindrance of o-methyl substituent restricts the access of the dopant, the helical structure in polymer backbone could not be formed. It is considered that the decreased doping level is an important contributing factor to the reduced crystallinity in POT.

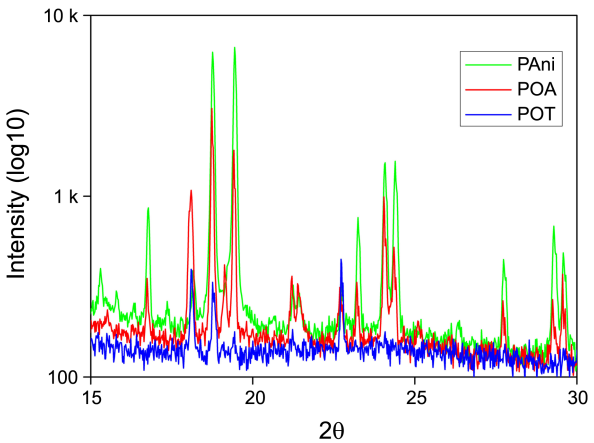

Figure 6. XRD patterns of PAni, POA, and POT films.

Conclusions

(+)-CSA doped PAni, POA, and POT films were formed by potentiodynamic electropolymerization. Steric effects caused by the substituent would influence the polymer conformation and the doping level, which in turn would determine their optical activity, morphology, and crystallinity. The methyl group in the *ortho* position of the phenyl ring in PAni resulted in greater steric hindrance than did the methoxy group. As the steric hindrance increased in the order of POT > POA > PAni, the doping level decreased.

Helical inversion of the polymer backbone was indicated by the CD bands of POA, but no CD bands were observed for POT. The formation of helical structure has had a noticeable effect on the crystallinity. The polymer morphology strongly depended on the nature and size of the substituent, and it changed from the rod-like PAni to the granular POA and fibrous POT.

Acknowledgments. We would like to thank Prof. Jang Myoun Ko (Hanbat Nat'l Univ.) for the kind advice on electrochemical analysis. And the publication cost of this paper was supported by the Korean Chemical Society.

References

1. Takano, N.; Seki, C. *Electrochemistry* **2006**, *74*, 596.
2. Pleus, S.; Schulte, B. *J. Solid State Electrochem.* **2001**, *5*, 522.
3. de Lacy Costello, B. P. J; Ratcliffe, N. M.; Sivanand, P. S. *Synth. Met.* **2003**, *139*, 43.
4. Kaniewska, M.; Sikora, T.; Kataky, R.; Trojanowicz, M. *J. Biochem. Biophys. Methods* **2008**, *70*, 1261.
5. Ogata, N. *Macromol. Symp.* **1997**, *118*, 693.
6. Ramos, J. C.; Souto-Maior, R. M.; Navarro, M. *Polymer* **2006**, *47*, 8095.
7. Majidi, M. R.; Kane-Maguire, L. A. P.; Wallace, G. G. *Polymer* **1994**, *35*, 3113.
8. Havinga, E. E.; Bouman, M. M.; Meijer, E. W.; Pomp, A.; Simenon, M. M. J. *Synth. Met.* **1994**, *66*, 93.
9. Ashraf, S. A.; Kane-Maguire, L. A. P.; Majidi, M. R.; Pyne, S. G.; Wallace, G. G. *Polymer* **1997**, *38*, 2627.
10. Yuan, G. L.; Liu, C.; Kuramoto, N.; Yang, Z. F. *Polym. Int.* **2010**, *59*, 1187.
11. Su, S. J.; Kuramoto, N. *Macromolecules* **2001**, *34*, 7249.
12. Yuan, G. L.; Kuramoto, N. *Macromolecules* **2003**, *36*, 7939.
13. Yan, Y.; Deng, K.; Yu, Z.; Wei, Z. X. *Angew. Chem.Int. Ed.* **2009**, *48*, 2003.
14. Su, S. J.; Takeishi, M.; Kuramoto, N. *Macromolecules* **2002**, *35*, 5752.
15. Anjum, M. N.; Zhu, L. H.; Luo, Z. H.; Yan, J. C.; Tang, H. Q. *Polymer* **2011**, *52*, 5795.
16. Majidi, M. R.; Kane-Maguire, L. A. P.; Wallace, G. G. *Polymer* **1995**, *36*, 3597.
17. Bhadra, S.; Khastgir, D. *Polym. Test.* **2008**, *27*, 851.
18. Yang, S. M.; Chiang, J. H. *Synth. Me.* **1991**, *41*, 761.
19. Patil, S.; Mahajan, J. R.; More, M. A.; Patil, P. P.; Gosavi, S. W.; Gangal, S. A. *Polym. Int.* **1998**, *46*, 99.
20. Hao, Q. L.; Lei, W.; Xia, X. F.; Yan, Z. Z.; Yang, X. J.; Lu, L. D.; Wang, X. *Electrochim. Acta* **2010**, *55*, 632.
21. Wei, Y.; Focke, W. W.; Wnek, G. E.; Ray, A.; Macdiarmid, A. G. *J. Phy. Chem.* **1989**, *93*, 495.
22. de Torresi, S. I. C.; Bassetto, A. N.; Trasferetti, B. C. *J. Solid State Electrochem.* **1998**, *2*, 24.
23. Athawale, A. A.; Kulkarni, M. V.; Chabukswar, V. V. *Mater. Chem. Phy.* **2002**, *73*, 106.
24. Sasaki, I.; Janata, J.; Josowicz, M. *Polym. Degrad. Stab.* **2007**, *92*, 1408.
25. Kulkarni, M. V.; Viswanath, A. K. *Eur. Polym. J.* **2004**, *40*, 379.
26. Kumar, P. R.; Kalpana, D.; Renganathan, N. G.; Pitchumani, S. *Electrochim. Acta* **2008**, *54*, 442.
27. Su, S. J.; Kuramoto, N. *Chem. Mater.* **2001**, *13*, 4787.
28. Jamal, R.; Abdiryim, T.; Ding, Y. J.; Nurulla, I. *J. Polym. Res.* **2008**, *15*, 75.
29. Leclerc, M.; D'Aprano, G.; Zotti, G. *Synth. Met.* **1993**, *55*, 1527.
30. Guo, H. L.; Knobler, C. M.; Kaner, R. B. *Synth. Met.* **1999**, *101*, 44.
31. Zhang, L. J.; Wan, M. X. *Thin Solid Films* **2005**, *477*, 24.
32. Yan, Y.; Yu, Z.; Huang, Y. W.; Yuan, W. X.; Wei, Z. X. *Adv. Mater.* **2007**, *19*, 3353.
33. He, C.; Tan, Y. W.; Li, Y. F. *J. Appl. Polym. Sci.* **2003**, *87*, 1537.
34. Raut, B. T.; Godse, P. R.; Pawar, S. G.; Chougule, M. A.; Bandgar, D. K.; Patil, V. B. *Measurement* **2012**, *45*, 94.
35. Varma, S. J.; Xavier, F.; Varghese, S.; Jayalekshmi, S. *Polym. Int.* **2012**, *61*, 743.